
This is an electronic reprint of the original article.
This reprint may differ from the original in pagination and typographic detail.

Li, Lifei; Zheng, Xinliang; Jin, Chenjie; Qi, Mei; Chen, Xiaoming; Ren, Zhaoyu; Bai, Jintao; Sun, Zhipei

High repetition rate Q-switched radially polarized laser with a graphene-based output coupler

Published in:
Applied Physics Letters

DOI:
[10.1063/1.4902917](https://doi.org/10.1063/1.4902917)

Published: 01/12/2014

Document Version
Publisher's PDF, also known as Version of record

Please cite the original version:
Li, L., Zheng, X., Jin, C., Qi, M., Chen, X., Ren, Z., ... Sun, Z. (2014). High repetition rate Q-switched radially polarized laser with a graphene-based output coupler. Applied Physics Letters, 105(22), 1-4. [221103]. DOI: 10.1063/1.4902917

This material is protected by copyright and other intellectual property rights, and duplication or sale of all or part of any of the repository collections is not permitted, except that material may be duplicated by you for your research use or educational purposes in electronic or print form. You must obtain permission for any other use. Electronic or print copies may not be offered, whether for sale or otherwise to anyone who is not an authorised user.

High repetition rate Q-switched radially polarized laser with a graphene-based output coupler

Lifei Li, Xinliang Zheng, Chenjie Jin, Mei Qi, Xiaoming Chen, Zhaoyu Ren, Jintao Bai, and Zhipei Sun

Citation: *Appl. Phys. Lett.* **105**, 221103 (2014); doi: 10.1063/1.4902917

View online: <https://doi.org/10.1063/1.4902917>

View Table of Contents: <http://aip.scitation.org/toc/apl/105/22>

Published by the [American Institute of Physics](#)

Articles you may be interested in

[Ultrafast all-fiber based cylindrical-vector beam laser](#)

Applied Physics Letters **110**, 021107 (2017); 10.1063/1.4973922

[Black phosphorus saturable absorber for ultrashort pulse generation](#)

Applied Physics Letters **107**, 051108 (2015); 10.1063/1.4927673

[Tungsten disulphide based all fiber Q-switching cylindrical-vector beam generation](#)

Applied Physics Letters **107**, 191108 (2015); 10.1063/1.4935465

[Fiber lasers generating radially and azimuthally polarized light](#)

Applied Physics Letters **93**, 191104 (2008); 10.1063/1.3023072

[Graphene Q-switched, tunable fiber laser](#)

Applied Physics Letters **98**, 073106 (2011); 10.1063/1.3552684

[Fiber laser generating switchable radially and azimuthally polarized beams with 140 mW output power at 1.6 \$\mu\text{m}\$ wavelength](#)

Applied Physics Letters **95**, 191111 (2009); 10.1063/1.3263724

Quantum Design Brings You the Next Generation Magneto-Optic Cryostat

Only be limited by your imagination...

Room Temperature Window
Split-Coil Conical Magnet
Sample Pod
User Wiring Ports

Learn More

Quantum Design
qdusa.com/opticool5

8 Optical Access Ports: 7 Side; 1 Top
Temperature Range: 1.7 K to 350 K
7 T Split-Coil Conical Magnet
Low Vibration: <10 nm peak-to-peak
89 mm x 84 mm Sample Volume
Automated Temperature & Magnet Control
Cryogen Free

High repetition rate Q-switched radially polarized laser with a graphene-based output coupler

Lifei Li,¹ Xinliang Zheng,^{2,a)} Chenjie Jin,¹ Mei Qi,¹ Xiaoming Chen,¹ Zhaoyu Ren,^{1,a)} Jintao Bai,^{1,2} and Zhipei Sun³

¹National Key Laboratory of Photoelectric Technology and Functional Materials (Culture Base), and Institute of Photonics and Photon-Technology, Northwest University, Xi'an 710069, China

²Department of Physics, Northwest University, Xi'an 710069, China

³Department of Micro- and Nanosciences, Aalto University, P.O. Box 13500, FI-00076 Aalto, Finland

(Received 16 August 2014; accepted 16 November 2014; published online 1 December 2014)

We demonstrate a Q-switched radially polarized all-solid-state laser by transferring a graphene film directly onto an output coupler. The laser generates Q-switched radially polarized beam (QRPB) with a pulse width of 192 ns and 2.7 W average output power. The corresponding single pulse energy is up to 16.2 μ J with a high repetition rate of 167 kHz. The M^2 factor and the polarization purity are ~ 2.1 and 96%, respectively. Our QRPB source is a simple and low-cost source for a variety of applications, such as industrial material processing, optical trapping, and microscopy. © 2014 AIP Publishing LLC. [<http://dx.doi.org/10.1063/1.4902917>]

Radially polarized beam (RPB), which possesses a unique polarization mode, is drawing more and more attention in the last 20 yr. Due to its intriguing properties (e.g., diffraction limit¹ and strong longitudinal electric field after focusing²), it can be widely applied for various applications, such as high-resolution microscopy,¹ material processing,^{2,3} electron acceleration,⁴ and optical trapping.⁵ In general, the generation methods of RPB can be mainly itemized into two categories: one is transformation of polarization state outside the laser cavity with special optical devices (e.g., spatially variable retardation plate⁶ or Mach-Zehnder interferometer⁷). Another one is polarization selection inside the laser cavity^{8–11} (e.g., employing a conical Brewster prism into the cavity to select RPB output⁸). Obviously, the intracavity approach is more compact and efficient, in contrast to its external-cavity counterpart. Combining the radial polarization control with Q-switching technology can produce large energy radially polarized pulses, which we believe is a vital step toward diversified application of RPB. However, thus far, few papers have been reported on Q-switched radially polarized beam (QRPB) from solid lasers: In 2007, Meier *et al.*¹² demonstrated the producing of QRPB with an acousto-optic modulator. But active Q-switching typically requires a fast electronic driver that makes the laser system complicated, and the output beam quality is not good enough (e.g., $\sim 80\%$ polarization purity and M^2 of ~ 2.3 ¹²) due to the existence of high-order transverse modes. Later in 2008, Li *et al.*¹³ reported a passively Q-switched microchip laser that emitted QRPB with Cr^{4+} :YAG crystal as the saturable absorber (SA). However, their output power is only 450 mW, which is mainly limited by the strong thermal lensing effect in Cr^{4+} :YAG and gain crystals.¹³ Therefore, it is crucial to explore and develop novel Q-switched radially polarized solid lasers with simpler configuration and better

performance (e.g., higher output power, better beam quality and polarization purity).

Recently, carbon nanotubes and graphene have been demonstrated as promising SAs^{14–17} with superior performance. Particularly, graphene has a number of distinctive advantages (e.g., inherent wide operation bandwidth^{18–20} and ultrafast recovery time²¹) over traditional SAs. These advantages, coupled with mechanical and environmental robustness,²¹ controllable modulation depth,²² and extremely high thermal conductivity,²¹ make graphene an excellent SA^{16,17,23} to mode-lock various lasers (e.g., fiber,^{15–17,23–26} solid-state,^{27–30} waveguide,³¹ and semiconductor²² lasers).

In this letter, we report a graphene-based Q-switched radially polarized all-solid-state laser. The graphene film is directly transferred on the output coupler mirror for Q-switching.^{31,32} This laser does not require any special polarization transformation or selection components, which makes the laser system compact, cost-effective, and versatile for various applications. The maximal average output power of QRPB is 2.7 W. The shortest pulse width is 192 ns with a pulse energy of 16.2 μ J and a repetition rate up to 167 kHz.

Our key device is the graphene-based output coupler (GOC), which is prepared as follows: First, we fabricate large-area and high-quality uniform graphene film by the atmospheric pressure chemical vapor deposition (APCVD) method. C_2H_2 served as the carbon precursor and Cu foil is used as the catalyst.^{33–35} This not only extends the size of the grains but also leads to very easy transfer.^{33–35} A $2 \times 2 \text{ cm}^2$ Cu foil (25 μm thick) was heated to 1000 °C under a $\text{Ar}:\text{H}_2:\text{C}_2\text{H}_2$ mixture with flow ratio 950:50:1. The grown time was set to 10 min and ultimately formed a graphene film on the Cu foil. It has been demonstrated that graphene grown under such conditions in our lab usually has a bilayer structure.³⁵ Then the film was cut into two pieces with $1 \times 2 \text{ cm}^2$ size and the Cu foil was etched out with $\text{Fe}(\text{NO}_3)_3$ solution. One piece of film was transferred onto a quartz plate for characterization and another one was transferred onto a plane output coupler (BK7 glass substrate) with a

^{a)}Authors to whom correspondence should be addressed. Electronic addresses: zhengxl@nwu.edu.cn and rzy@nwu.edu.cn

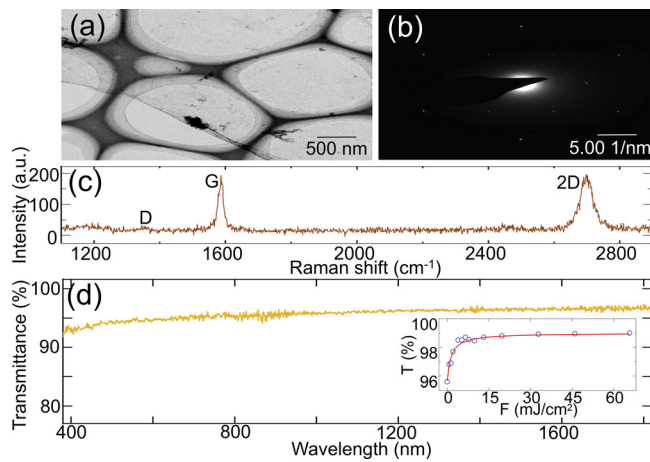


FIG. 1. (a) HRTEM image, (b) SEAD pattern, (c) Raman spectrum, and (d) transmittance of the graphene film. The inset shows the nonlinear absorption property of graphene.

transmittance of 10% at 1064 nm for lasing. Figures 1(a) and 1(b) illustrate the high-resolution transmission electron microscopy (HRTEM) image and the selected electron diffraction (SEAD) pattern of the graphene film, respectively, indicating our graphene has an excellent crystallization degree. The Raman spectrum was acquired with a 514-nm laser as shown in Fig. 1(c). Note that the D-peak (also known as defect peak³⁶) is almost neglectable, which suggests that there are negligible defects in our graphene.³⁶ The transmittance of our graphene was measured with a UV-NIR spectrophotometer (Lambda 920, Perkin-Elmer), as shown in Fig. 1(d). The transmittance of graphene is $\sim 95.5\%$ at 1064 nm, which corresponds to $\sim 89\%$ and $\sim 93.2\%$ transmittance measured for graphene on quartz plate and pure quartz plate, respectively. It proves that the number of graphene layers is two (i.e., $\sim 2.3\%$ absorbance per layer^{29,37}). The nonlinear optical absorption property of our graphene was measured with a 1064-nm pulsed laser (150 ns pulse width, 10 KHz repetition rate). The results are shown in the inset of Fig. 1(d). The non-saturable loss is $\sim 1\%$.

Fig. 2(a) illustrates the experimental setup of our graphene-based Q-switched radially polarized solid laser. A

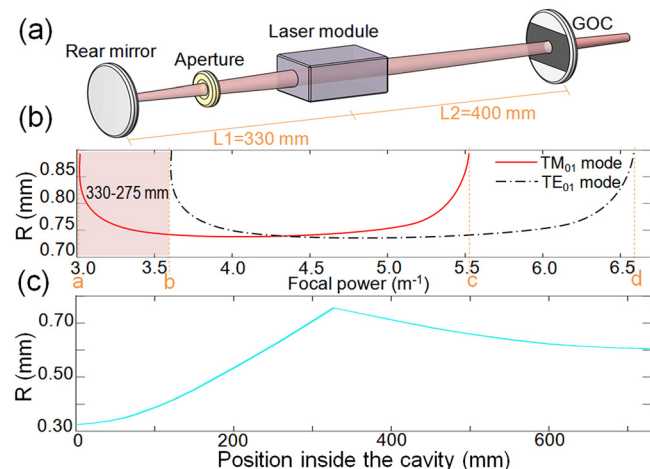


FIG. 2. (a) Laser setup. (b) Beam radius (R) versus the focal power ($1/f_r$) at the principal plane of laser rod. (c) Beam radius as a function of position within the cavity. The cavity position starts from the rear mirror to the GOC.

commercial diode-side-pumped Nd:YAG laser module (rod size, 2 mm in diameter and 45 mm long; dopant, 0.6%; [111]-cut) was installed in a simple cavity, which is specially designed in a highly robust and compact linear Fabry-Pérot cavity configuration. A high-reflectivity plane mirror ($R > 99.9\%$ at 1064 nm, Rear mirror) and the fabricated GOC ($T \sim 9.5\%$ at 1064 nm with graphene) were, respectively, located at a distance of $L_1 = 330$ mm and $L_2 = 400$ mm from the middle of the laser module. An aperture with 1 mm diameter was located 180 mm far away from the rear mirror to limit the high-order transverse modes and thus improve the radial polarization quality. Such a half-symmetric cavity configuration was particularly designed to allow the QRPB output based on the thermal birefringence and bifocal thermal lensing of the side-pumped Nd:YAG rod.^{9,10} The stability zone condition of the cavity can be analyzed by using the ray transfer matrix method.³⁸ Since the radially thermal focal length f_r is typically shorter than the azimuthally thermal focal length f_a in a Nd:YAG rod (i.e., $f_a/f_r = 1.2$ ³⁹), the stable region of azimuthally polarized mode (TE_{01} mode) always shifts compared to that of radially polarized mode (TM_{01} mode). As a result, it is possible to have only TM_{01} mode stably operating on the edge of the stable region.¹⁰ Based on this, we intentionally designed the laser operation in TM_{01} mode by selecting suitable cavity length (i.e., $L_1 = 330$ mm, $L_2 = 400$ mm), after taking account of Q-switching (i.e., relatively short cavity length to facilitate Q-switching operation⁴⁰). Our cavity operates stably when the thermal focal length of the Nd:YAG rod (note that the Nd:YAG rod acts as a bifocal thermal lens with f_a, f_r two thermal focal lengths) meets the stability zone condition (i.e., 330–180 mm). Fig. 2(b) describes the calculated beam radius versus the focal power ($1/f_r$) at the principal plane of Nd:YAG rod. The stable region of TE_{01} mode shifts, because $f_a/f_r = 1.2$, as discussed. A radially polarized beam starts to oscillate because f_r (i.e., 330–275 mm) first meets the stability zone condition, while the azimuthally polarized beam is blocked as f_a (i.e., 396–330 mm) is larger than what is required for the stability zone condition. Region “ab” (marked in pink, the corresponding f_r is between 330–275 mm) is the regime where only the TM_{01} mode is stable. The thermal focal length (both f_r and f_a) decreases with the pump power. Once f_r is decreased to 275 mm (the corresponding focal power is $\sim 3.6 \text{ m}^{-1}$) with the increase of pump power, the azimuthally polarized beam will also start to oscillate because f_a is 330 mm at this time (which starts to meet the stability zone condition), and the laser will operate in the overlap zone (i.e., the region “bc”) of the TM_{01} and TE_{01} modes with multimode output. Fig. 2(c) shows the beam radius ($1/e^2$) of the TM_{01} mode versus the position within the cavity at f_r of 300 mm. The mode volume was maximal at the position of the gain medium to maximize the output power, while maintaining relative large beam radius (~ 0.6 mm) on the GOC to minimize the incident intensity on our graphene device to suppress the mode-locking for high power Q-switching operation.⁴¹

The output power was monitored via a power meter (FieldMaxII, Coherent), as depicted in Fig. 3. As soon as the drive current exceeded the threshold of 15.3 A (which corresponds to ~ 330 mm thermal focal length measured for TM_{01}

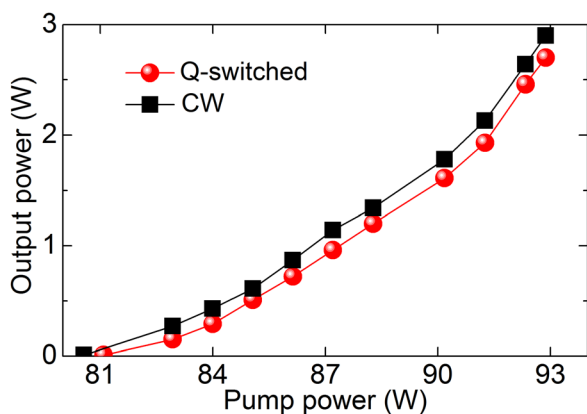


FIG. 3. Output power versus pump power for Q-switched and CW operation.

mode by a He-Ne laser), the QRPB was obtained. The maximum output power was 2.7 W with a drive current of 17.2 A (which corresponds to ~ 300 mm thermal focal length measured for TM_{01} mode). It should be pointed out that the drive current was changed from 15.3 to 17.2 A corresponding to the pump power change from 81.1 to 92.8 W. The electro-optical efficiency of our laser module is $\sim 50\%$. In order to complete the thermal polarization selection in a relatively short cavity, the laser has to operate with relatively high threshold condition. The slope efficiency is approximately 23%. During the experiment, we replaced the GOC by an original output coupler (i.e., an output coupler without graphene film, $T = 10\%$) to measure the continuous-wave (CW) output performance for comparison. The CW output power curve is also plotted in Fig. 3. With a same drive current of 17.2 A (corresponding to pump power of 92.8 W), 2.9 W CW RPB was obtained. Note that the ratio of the output power between Q-switched and CW operations reaches a high value of 0.93, showing the low non-saturable loss of our graphene thanks to its high quality. Using a photoelectric detector (FGA21, Thorlabs) and a 1-GHz bandwidth oscilloscope (DSO7052A, Agilent), the pulse characteristics of the output QRPB were investigated. With the increase of pump power, the pulse width decreased quickly while the repetition rate increased nearly linearly just as expected, which is a typical feature of passively Q-switched lasers. This is because the saturation frequency of graphene was increased with the increase of cavity gain. The detailed variations of the pulse width and repetition rate as functions of pump power are shown in Fig. 4(a). We obtained the shortest pulse width of 192 ns at the maximum output power of 2.7 W. The single pulse envelope and pulse train are shown in

Fig. 4(b). The corresponding repetition rate was up to 167 kHz, which is much higher than those of previously published Q-switched radially polarized solid lasers (e.g., 1.56¹² and 6.7¹³ kHz). The pulse energy was calculated to be 16.2 μ J, comparable to previously reported graphene-based Q-switched lasers (e.g., 18 μ J⁴² for fiber lasers and 13.5 μ J⁴³ for solid lasers). Further increasing the pump power, the pulses became unstable possibly due to the super-saturation of SA.^{40,42} Currently, further exploration (e.g., increasing the beam size on our graphene device or adjusting the number of graphene layer) to optimize the laser cavity is under way to improve the output power and obtain Q-switched azimuthally polarized beam (designed, and marked as the region “cd” in Fig. 2(b)).

The polarization property of QRPB is crucial for various applications. The output polarization performance was analyzed by placing a linear polarizer perpendicularly in front of a camera. Fig. 5(a) shows the beam profile without the polarizer. A dark spot appeared at the center of the beam, which is clearly discerned as the TM_{01} mode for the expected QRPB. Figures 5(b) and 5(c) exhibit the beam profile after transmitting through a linear polarizer rotated at horizontal and vertical directions, respectively. It is apparent that the dark bands between the bimodal intensity patterns are perpendicular to the directions of the polarizer (indicated by the double-arrows), and this feature verifies that the laser beam is indeed radially polarized. Fig. 5(d) shows the measured intensity distribution curve along the radial direction of the doughnut-shaped beam profile in Fig. 5(a). Radial polarization can be regarded as a superposition of linear polarization along all the radial directions on the beam cross section. Therefore, when the QRPB was incident on a small size aperture (here we used an aperture with 200 μ m diameter) placed far away from the GOC, the leakage light passing through the aperture can be considered to be linearly polarized and its polarization degree can represent approximately that of the whole beam.¹³ Based on this principle,¹³ the polarization extinction ratio (PER) of the leakage light was measured to be 49:1, which corresponds to 96% polarization purity. It is comparable to those of previously published Q-switched radially polarized solid lasers.¹³ In addition, the M^2 factor was also measured to be ~ 2.1 (i.e., $M_x^2 = 2.13$, $M_y^2 = 2.07$) with a beam analyzer (Nanoscan, Photon) as shown in Fig. 5(e). This is close to the theoretical value of 2 expected for TM_{01} mode,⁴⁴ which reveals the high beam quality of our QRPB.

In conclusion, we have demonstrated the first graphene-based Q-switched radially polarized laser. The high quality QRPB with 16.2 μ J pulse energy and 167 kHz repetition rate was established. Our laser is a simple, reliable, and practical

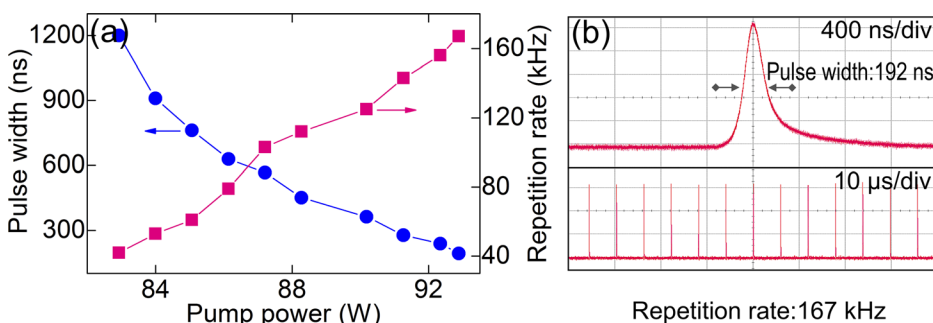


FIG. 4. (a) Pulse width and repetition rate as functions of pump power. (b) Oscilloscope traces of single pulse envelope and pulse train at the maximum output power of 2.7 W.

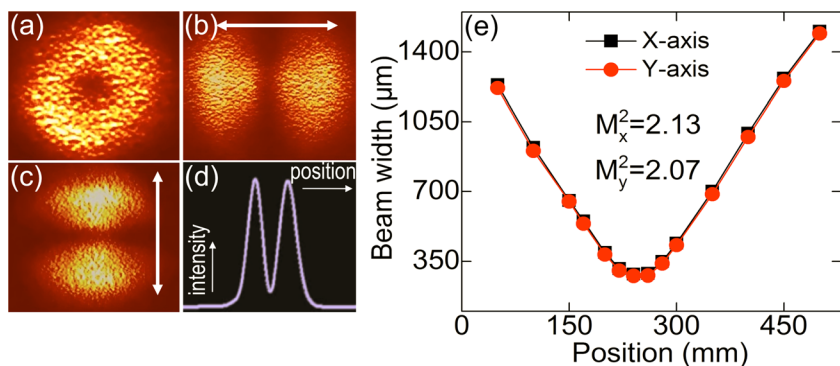


FIG. 5. (a) Beam profile of the QRPB without the polarizer. (b) and (c) Beam profile after the polarizer with horizontal and vertical directions (indicated by double-arrows). (d) Intensity distribution along the radial direction of the doughnut-shaped beam profile. (e) M^2 factor measurement result.

QRPB source, which can be potentially applied in various applications such as material processing and microscopy.

This research is sponsored by the ICP (201410780), 973 Plan of China (2012CB723407), NSFC (61275105, 61177059), NSF (2012JM1019), EBF (11JS106) of Shaanxi Province, Teknologiateollisuus TT-100, the European Union's Seventh Framework Programme (REA Grant Agreement No. 631610), Academy of Finland and Aalto University (Finland).

¹R. Dorn, S. Quabis, and G. Leuchs, *Phys. Rev. Lett.* **91**, 233901 (2003).
²L. Novotny, M. R. Beversluis, K. S. Youngworth, and T. G. Brown, *Phys. Rev. Lett.* **86**, 5251 (2001).
³V. G. Niziev and A. V. Nesterov, *J. Phys. D: Appl. Phys.* **32**, 1455 (1999).
⁴D. N. Gupta, N. Kant, D. E. Kim, and H. Suk, *Phys. Lett. A* **368**, 402 (2007).
⁵T. Kuga, Y. Torii, N. Shiokawa, T. Hirano, Y. Shimizu, and H. Sasada, *Phys. Rev. Lett.* **78**, 4713 (1997).
⁶G. Machavariani, Y. Lumer, I. Moshe, A. Meir, and S. Jackel, *Opt. Lett.* **32**, 1468 (2007).
⁷N. Passilly, R. S. Denis, K. Ait-Ameur, F. Treussart, R. Hierle, and J. Roch, *J. Opt. Soc. Am. A* **22**, 984 (2005).
⁸Y. Kozawa and S. Sato, *Opt. Lett.* **30**, 3063 (2005).
⁹I. Moshe, S. Jackel, and A. Meir, *Opt. Lett.* **28**, 807 (2003).
¹⁰A. Ito, Y. Kozawa, and S. Sato, *J. Opt. Soc. Am. B* **26**, 708 (2009).
¹¹Z. Fang, K. Xia, Y. Yao, and J. Li, *IEEE J. Sel. Top. Quantum Electron.* **21**, 1 (2015).
¹²M. Meier, V. Romano, and T. Feurer, *Appl. Phys. A* **86**, 329 (2007).
¹³J. Li, K. Ueda, M. Musha, L. Zhong, and A. Shirakawa, *Opt. Lett.* **33**, 2686 (2008).
¹⁴S. Y. Set, H. Yaguchi, Y. Tanaka, and M. Jablonski, *IEEE J. Sel. Top. Quantum Electron.* **10**, 137 (2004).
¹⁵T. Hasan, Z. Sun, F. Bonaccorso, P. H. Tan, A. G. Rozhin, and A. C. Ferrari, *Adv. Mater.* **21**, 3874 (2009).
¹⁶Q. Bao, H. Zhang, Y. Wang, Z. Ni, Z. X. Shen, K. P. Loh, and D. Y. Tang, *Adv. Funct. Mater.* **19**, 3077 (2009).
¹⁷A. Martinez and Z. Sun, *Nat. Photonics* **7**, 842 (2013).
¹⁸Z. Sun, D. Popa, T. Hasan, F. Torrisi, F. Wang, E. Kelleher, J. Travers, V. Nicolosi, and A. C. Ferrari, *Nano Res.* **3**, 653 (2010).
¹⁹B. Fu, Y. Hua, X. Xiao, H. Zhu, Z. Sun, and C. Yang, *IEEE J. Sel. Top. Quantum Electron.* **20**, 1100705 (2014).
²⁰D. Popa, Z. Sun, T. Hasan, F. Torrisi, F. Wang, and A. C. Ferrari, *Appl. Phys. Lett.* **98**, 073106 (2011).

²¹F. Bonaccorso, Z. Sun, T. Hasan, and A. C. Ferrari, *Nat. Photonics* **4**, 611 (2010).
²²C. A. Zaugg, Z. Sun, V. J. Wittwer, D. Popa, S. Milana, T. S. Kulmala, R. S. Sundaram, M. Mangold, O. D. Sieber, M. Golling *et al.*, *Opt. Express* **21**, 31548 (2013).
²³Z. Sun, T. Hasan, F. Torrisi, D. Popa, G. Privitera, F. Wang, F. Bonaccorso, D. M. Basko, and A. C. Ferrari, *ACS Nano* **4**, 803 (2010).
²⁴H. Zhang, D. Y. Tang, L. M. Zhao, Q. L. Bao, and K. P. Loh, *Opt. Express* **17**, 17630 (2009).
²⁵D. Popa, Z. Sun, F. Torrisi, T. Hasan, F. Wang, and A. C. Ferrari, *Appl. Phys. Lett.* **97**, 203106 (2010).
²⁶A. Martinez and S. Yamashita, *Appl. Phys. Lett.* **101**, 041118 (2012).
²⁷W. D. Tan, C. Y. Su, R. J. Knize, G. Q. Xie, L. J. Li, and D. Y. Tang, *Appl. Phys. Lett.* **96**, 031106 (2010).
²⁸L. Li, Z. Ren, X. Chen, M. Qi, X. Zheng, J. Bai, and Z. Sun, *Appl. Phys. Express* **6**, 082701 (2013).
²⁹A. A. Lagatsky, Z. Sun, T. S. Kulmala, R. S. Sundaram, S. Milana, F. Torrisi, O. L. Antipov, Y. Lee, J. H. Ahn, C. T. A. Brown *et al.*, *Appl. Phys. Lett.* **102**, 013113 (2013).
³⁰S. D. D. Cafiso, E. Ugolotti, A. Schmidt, V. Petrov, U. Griebner, W. B. Cho, F. Rotermund, S. Bae, B. H. Hong, G. Reali *et al.*, *Opt. Lett.* **38**, 1745 (2013).
³¹R. Mary, G. Brown, S. J. Beecher, F. Torrisi, S. Milana, D. Popa, T. Hasan, Z. Sun, E. Lidorikis, S. Ohara *et al.*, *Opt. Express* **21**, 7943 (2013).
³²P. M. Hernando, J. M. Guerra, and R. Weigand, *Laser Phys.* **23**, 025003 (2013).
³³X. Li, W. Cai, J. An, S. Kim, J. Nah, D. Yang, R. Piner, A. Velamakanni, I. Jung, E. Tutuc *et al.*, *Science* **324**, 1312 (2009).
³⁴F. Bonaccorso, A. Lombardo, T. Hasan, Z. Sun, L. Colombo, and A. C. Ferrari, *Mater. Today* **15**, 564 (2012).
³⁵M. Qi, Z. Ren, Y. Jiao, Y. Zhou, X. Xu, W. Li, J. Li, X. Zheng, and J. Bai, *J. Phys. Chem. C* **117**, 14348 (2013).
³⁶A. C. Ferrari, J. C. Meyer, V. Scardaci, C. Casiraghi, M. Lazzeri, F. Mauri, D. Jiang, K. S. Novoselov, S. Roth, and A. K. Geim, *Phys. Rev. Lett.* **97**, 187401 (2006).
³⁷R. R. Nair, P. Blake, A. N. Grigorenko, T. Stauber, N. M. R. Peres, and A. K. Geim, *Science* **320**, 1308 (2008).
³⁸H. Kogelnik and T. Li, *Appl. Opt.* **5**, 1550 (1966).
³⁹W. Koehner, *Solid-State Laser Engineering* (Springer, 2005), p. 444.
⁴⁰G. J. Spühler, R. Paschotta, R. Fluck, B. Braun, M. Moser, G. Zhang, E. Gini, and U. Keller, *J. Opt. Soc. Am. B* **16**, 376 (1999).
⁴¹F. X. Kärtner, L. R. Brovelli, D. Kopf, M. Kamp, I. Calasso, and U. Keller, *Opt. Eng.* **34**, 2024 (1995).
⁴²Y. Tang, X. Yu, X. Li, Z. Yan, and Q. Wang, *Opt. Lett.* **39**, 614 (2014).
⁴³R. Zhou, P. Tang, Y. Chen, S. Chen, C. Zhao, H. Zhang, and S. Wen, *Appl. Opt.* **53**, 254 (2014).
⁴⁴D. Deng, X. Fu, C. Wei, J. Shao, and Z. Fan, *Appl. Opt.* **44**, 7187 (2005).